

Absence of an insulator-metal transition in Rb_4C_{60} up to 2 GPa

Agnieszka Iwasiewicz-Wabnig,* Thomas Wågberg, Tatiana L. Makarova, and Bertil Sundqvist
Department of Physics, Umeå University, S-901 87 Umeå, Sweden

(Received 23 August 2007; revised manuscript received 24 October 2007; published 29 February 2008)

We present the results of direct resistance measurements on Rb_4C_{60} under pressures up to 2 GPa. At all pressures covered by this study and over the temperature range of 90–450 K Rb_4C_{60} is a semiconductor with a weakly pressure dependent band gap near 0.7 eV. We do not observe the insulator-to-metal transition previously reported to occur below 1.2 GPa, although we cannot rule out the possibility that such a transition might occur at some significantly higher pressure. The measured resistivity is surprisingly low and is dominated by carriers excited over a 0.1 eV gap. Because the corresponding conductivity increases with deformation of the sample, we assign these states to structural or orientational defects. The known structural transformation below 0.5 GPa leads to a decrease in resistivity under high pressure, but the material remains semiconducting. A Rb_6C_{60} control sample showed a similar behavior, also being a semiconductor under all conditions studied. At temperatures above 460 K, Rb was partially lost from our samples, resulting in metalization by a transformation into Rb_3C_{60} .

DOI: [10.1103/PhysRevB.77.085434](https://doi.org/10.1103/PhysRevB.77.085434)

PACS number(s): 72.80.Rj, 71.30.+h, 71.20.Tx, 62.50.-p

I. INTRODUCTION

Fullerenes, like other carbon materials, are easily doped (intercalated) by alkali metals (A). Early studies showed that well defined structural phases $A_x\text{C}_{60}$ with $x=1, 3, 4,$ and 6 could be synthesized by intercalation,^{1–3} and that the insertion of alkali metals was associated with a charge transfer of one electron per metal ion to the fullerene molecules. Because the conduction band of C_{60} can accept six electrons, C_{60} and A_6C_{60} were expected to be insulators and the intermediate phases should be metals. The A_3C_{60} compounds with half-filled bands were indeed found to be metallic,¹ and even superconducting,^{4,5} but the A_4C_{60} compounds^{2,6} turned out to be nonmetallic. Doping experiments on thin films⁷ show that, in general, the resistivity ρ of A_4C_{60} is about an order of magnitude higher than that of the corresponding A_3C_{60} material, and that the temperature coefficient of ρ is negative, indicating the presence of an energy gap in the band structure. The resistivities of the A_6C_{60} compounds are about another order of magnitude higher.

The nonmetallic behavior of the A_4C_{60} compounds remains a poorly understood phenomenon. Compared to the face centered cubic A_3C_{60} compounds, the lattices of the heavy alkali A_4C_{60} materials are slightly expanded to accommodate the extra metal ions, forming body centered tetragonal structures,^{2,6} while for the light alkali metals Li (Ref. 8) and Na (Ref. 9), and mixtures of these,¹⁰ doping to $x=4$ leads to charge-transfer induced fullerene polymerization into two unique lattices. For the nonpolymerized heavy alkali compounds, simple band structure calculations indicate that they should be metals, and the observed behavior is usually attributed to a gap induced by a strong Jahn-Teller effect.^{11–13}

Because of the poor understanding of the band structures of the heavy alkali metal A_4C_{60} compounds, a large interest was sparked by a report that high pressure ^{13}C NMR measurements on Rb_4C_{60} indicated a transformation into a metallic state at a pressure below 1.2 GPa.¹⁴ Although pure C_{60} has been very well investigated under pressure,^{15,16} much less is known about doped fullerenes under such conditions.

However, several recent high pressure studies have noted anomalies in the compression behavior^{17,18} and band structure¹⁹ of Rb_4C_{60} below 1 GPa, but no clear indications of an electronic transition have been found and many questions remain. We have therefore carried out direct measurements of the electric resistance on well characterized Rb_4C_{60} samples under pressures up to 2 GPa in the range of 90–500 K. The data reported below clearly show that *no insulator-metal transition occurs in Rb_4C_{60} over this range in temperature and pressure*, and that a standard semiconductor model can be fitted to the data for resistance versus temperature at all pressures. On heating to above 470 K, we actually do observe formation of a metallic phase, but we show that this is due to loss of Rb and formation of Rb_3C_{60} .

II. EXPERIMENTAL DETAILS

A. Sample synthesis and characterization

It is notoriously difficult to synthesize Rb_4C_{60} in pure form.^{3,17,19} Initial attempts at direct synthesis from stoichiometric amounts of Rb and C_{60} by the method of Kuntscher *et al.*²⁰ resulted in three-phase Rb_xC_{60} mixtures, and we have therefore produced our samples by the commonly used two-step method.^{2,21}

Fully intercalated Rb_6C_{60} was first produced by the standard vapor transport method. A known amount of sublimed C_{60} with a nominal purity of 99.98% (Term-USA, Berkeley, CA), heat treated for at least 12 h in a dynamical vacuum at 200 °C to remove water, oxygen, and other impurities, was inserted into one end of a glass tube, with an excess amount of metallic rubidium in the other end. The tube, which had a constriction in the middle to separate the two materials, was sealed under vacuum and inserted into a two-zone oven. Treatment at average temperatures of 250–300 °C for 2–4 weeks, with a temperature difference of 15–30 °C between the C_{60} and the rubidium to avoid unwanted distillation of the metal into the fullerene chamber, resulted in formation of well intercalated Rb_6C_{60} . Formation of a new

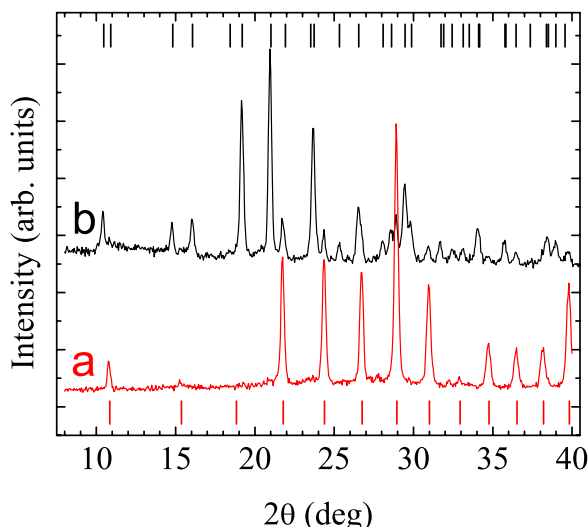


FIG. 1. (Color online) X-ray diffraction data for (a) Rb_6C_{60} precursor (red) and (b) nominal Rb_4C_{60} (black) from the same production batch as used in the high-pressure experiments (curves shifted vertically for clarity). Ticks show line positions for Rb_6C_{60} (bottom, red) and Rb_4C_{60} (top, black) calculated from literature data (Ref. 22).

phase was evident by a color change of the C_{60} powder from brownish black to silvery gray, and the weight of the Rb_6C_{60} samples usually indicated an error of less than 0.5% in the final stoichiometry. The material was also characterized by x-ray diffraction and Raman spectroscopy, with samples encased in glass capillaries. Typical results are shown in Figs. 1 and 2 [curve (a)].

Suitable amounts of Rb_6C_{60} and pure C_{60} were then well mixed and again sealed into a glass tube under vacuum. Be-

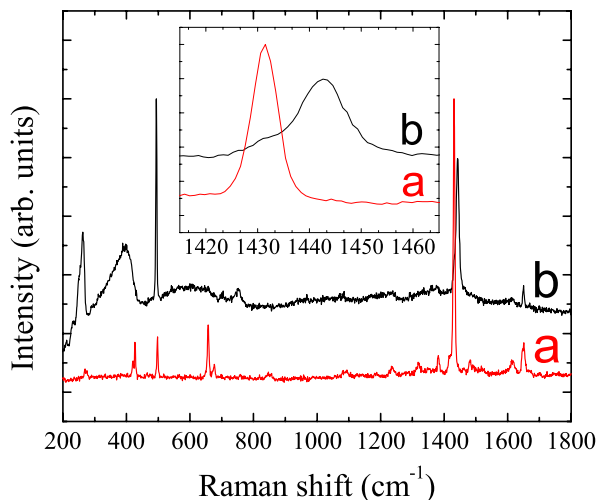


FIG. 2. (Color online) Raman spectra for (a) Rb_6C_{60} precursor (red) and (b) Rb_4C_{60} (black) from the same sample batch as used in the high-pressure studies, scaled and shifted vertically for easier comparison. Inset shows the $A_g(2)$ mode on an expanded energy scale. The broad, “triangular” feature between 300 and 420 cm^{-1} on curve (b) is due to an unknown impurity in the spectrometer itself.

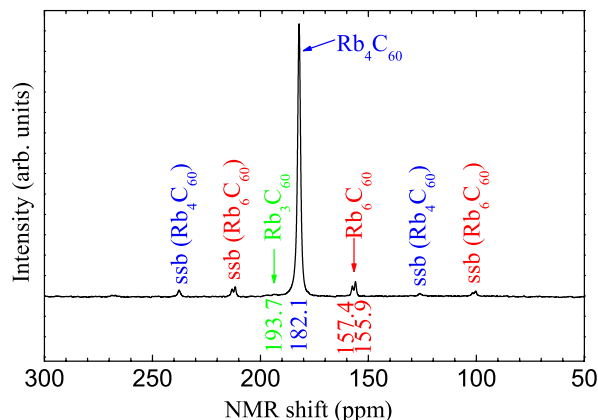


FIG. 3. (Color online) NMR spectrum of a nominal Rb_4C_{60} sample from the same batch as the samples used for resistance measurements. Rb_4C_{60} is clearly a majority phase, with small amounts of Rb_6C_{60} and traces of Rb_3C_{60} present (as labeled).

cause we wanted to detect transitions into a metallic state, we tried to avoid the initial presence of metallic Rb_3C_{60} in our samples, and we thus aimed for an overall stoichiometry of about $\text{Rb}_{4.1}\text{C}_{60}$ to obtain a material containing Rb_4C_{60} as majority phase and Rb_6C_{60} as minority phase.³ Since the latter should have a resistivity at least an order of magnitude higher than that of Rb_4C_{60} ,^{7,23} and since it has no known high pressure transitions, its presence should pose no serious problems. The mixtures were then annealed for another 2–4 weeks at 300–350 °C, after which the material was again characterized. Results from x-ray diffraction (XRD), Raman, and NMR measurements on typical samples taken from a single batch of material are shown in Figs. 1–3. The XRD results in Fig. 1 [curve (b)] clearly indicate that the majority phase is Rb_4C_{60} , but also shows a few percent of Rb_6C_{60} , as expected. Raman spectroscopy [Fig. 2, curve (b)] indicated that at least the surfaces of most grains were homogeneous, i.e., “pure” Rb_4C_{60} or Rb_6C_{60} , but in some cases also showed mixed phases. NMR is a powerful analysis tool, both because it probes the bulk of the material and because the three compounds discussed give well separated, sharp NMR lines.^{24,25} The NMR results in Fig. 3 indicated that the particular sample studied by this method was almost 100% pure Rb_4C_{60} . In most of our samples, none of the methods used could detect the presence of Rb_3C_{60} ; however, in a few cases, Raman studies could not rule out a small amount of surface Rb_3C_{60} .

Because both rubidium and the synthesized samples are very sensitive to oxidation, the synthesis as well as all subsequent storage and handling of the samples, including filling into the pressure cells, were carried out in an argon-filled glovebox with normal oxygen and water levels well below 1 ppm, or in closed glass capillaries.

B. Equipment and techniques

The high-pressure studies on Rb_4C_{60} were performed in three experiments, each on a different sample but with all samples taken from the batch of material characterized as

Rb_4C_{60} in Figs. 1–3. High pressure was applied in a piston-cylinder device with an internal diameter of 45 mm. Pressure calibration was performed in a separate, earlier experiment, calibrating oil pressure in the hydraulic press against a previously calibrated Manganin pressure gauge.

In each experiment, a few milligrams of Rb_4C_{60} powder were loaded into a Teflon pressure cell. The actual mass of each sample was not measured since the cell had to be loaded in a glovebox and the amount of material in each case was very small. To define the sample geometry and minimize extrusion and deformation on application of pressure, the powder was placed in shallow grooves, about 10×1.7 mm and 0.5 mm deep, machined either in a machinable glass ceramic (Macor™) sample holder (first experiment) or directly in the thick bottom of the Teflon cell (second and third experiments). All components expected to be in contact with the sample material were well dried. Before loading the samples, electric contacts made from 0.2 mm Nickel 200 wires were placed in the grooves in such a way as to enable four-pole resistance measurements, taking care to avoid shorting the current and voltage contacts. The powder was slightly compressed on to these contacts before the final filling of the pressure cell. Thicker Cu wires, leading out through the bottom gaskets, were soldered to the Ni contact wires a few millimeters from the samples.

The samples were finally covered with vacuum dried hexagonal BN, acting as a quasihydrostatic pressure transmitting medium. In the first experiment (using the ceramic holder), the cell was then filled up with dried talc powder, as in our recent studies of $\text{C}_{60}\text{C}_8\text{H}_8$,²⁶ while in the second and third experiments, a 2 mm thick Teflon plate was placed on top. On this plate, a planar Kanthal wire resistive heater was placed to allow fairly rapid temperature adjustments over a wide range. Slow cooling was provided by direct application of liquid nitrogen to the outside of the pressure vessel, which was insulated using standard mineral wool insulation. The temperature of the samples was monitored by a type *K* thermocouple placed in the pressure cell at a position geometrically equivalent to the position of the samples. The total temperature range achievable with this setup was from 90 to about 500 K.

In the two last experiments, two samples were investigated in each pressure run. One of these was always the pure Rb_4C_{60} , as discussed above, while the second one was either Rb_6C_{60} or a mixture of the Rb_xC_{60} compounds with $x=3, 4,$ and 6 for comparison. However, for reasons discussed below, the data for these samples did not add much useful information.

In all experiments, the resistance was measured continuously at intervals of 10–60 s, both while the pressure was changed during isothermal runs at or near room temperature and during isobaric temperature scans at selected pressures. At each pressure the resistance was studied over the widest possible temperature ranges to enable us to identify the conduction mechanism(s) in the materials studied. Each cooling and/or heating cycle down to liquid nitrogen temperatures took about 24 h, while high-temperature cycles above 300 K usually took 2–4 h. Each high pressure experiment lasted several days, the shortest just over a week, the longest for 3 weeks.

Finally, we note here that in the experiments where the pressure cell was filled with Teflon, we clearly observed the well known phase transitions of this material: (i) at about 300–360 K, on heating and/or cooling at pressures below 0.5 GPa, and (ii) a less visible transition, during room temperature pressure runs between 0.5 and 1 GPa.²⁷ The volume change involved gave a minor anomaly in the observed resistance of our samples (see Fig. 6 below), while the heat released (or absorbed) at the transition temporarily modified the heating and/or cooling rates.

As already mentioned above, the samples were characterized using (i) magic angle spinning NMR spectroscopy with single pulses at a 7 kHz spin rate using a Bruker AMX2 500, (ii) x-ray diffraction in a Siemens/Bruker 5000D powder diffractometer in θ - 2θ geometry, using Cu $K\alpha$ radiation, and (iii) Raman spectroscopy using a Renishaw 1000 micro-Raman spectrometer, with three excitation lasers (514.5, 632.5, and 780 nm) at powers of 0.2–2.0 mW. The magnetic measurements reported in Sec. III B were carried out using a Quantum Design MPMS XL superconducting quantum interference device (SQUID) magnetometer.

III. EXPERIMENTAL RESULTS AND DISCUSSION

A. Electrical resistance studies under pressure

1. Resistance versus pressure

We present first the qualitative behavior of the measured resistance as a function of pressure at room temperature. Based on the results of earlier pressure studies,^{14,17–19} we had expected to observe a rather sudden order-of-magnitude drop in the observed resistance at an insulator-metal transition somewhere in the range of 0.3–0.8 GPa at room temperature. If such an anomaly would be associated with a first-order structural transition, as suggested by Sabouri-Dodaran *et al.*,¹⁷ it might be rather sluggish, and to assure that there was time for a possible phase transition to occur, we always increased the pressure in small steps, allowing time for the sample to relax. However, in no experiment did we increase pressure continuously from 0 to 2 GPa. Instead, we increased pressure slowly in wide steps, stopping for 24 h at a time to carry out isobaric temperature scans at selected pressures. When returning to the initial temperature after each such scan the magnitude of the resistance had usually decreased by some small fraction. We will discuss the temperature and time dependence of the resistance in the following sections and concentrate here on the pressure dependence at room temperature.

As already mentioned above, in every experiment, the material was initially in powder form. The application of high pressure thus resulted in a rapid initial compression and large changes in effective sample dimensions. We are thus unable to report accurate data for the resistivity ρ and the analysis will be based only on the measured resistance R . However, for all phases identified, resistivity values based on the measured resistances and reasonable estimates of the geometrical parameters were compatible with literature data.^{7,23,28} As expected, during the initial compression of the samples, the measured resistance dropped drastically. An ex-

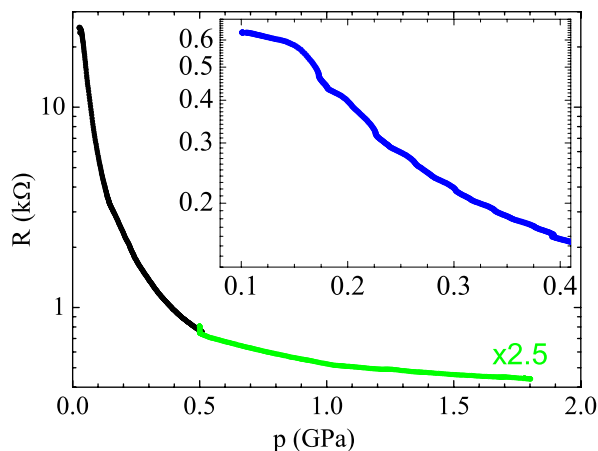


FIG. 4. (Color online) Resistance versus pressure at room temperature for the third Rb_4C_{60} sample up to 1.8 GPa. The high-pressure data have been multiplied by a constant to make the curve continuous through 0.5 GPa, where an extended temperature run was made. Inset shows data over the range of 0.1–0.4 GPa for the second sample (blue, see text).

ample of such a behavior is shown in Fig. 4 (first application of pressure in the third experiment). The curve shown in the figure exhibits a gradual change in slope just above 0.1 GPa. We assume that the steeper slope below this pressure is connected mainly with the initial compression of the powder into a solid film, while the more gentle variation at higher pressures is a real, intrinsic effect. For all initially Rb_4C_{60} samples studied, we observed a tendency for a “shelf” structure around 0.15 GPa, with a stronger slope setting in above about 0.17 GPa. In the first two experiments, we stopped the pressure increase already at 0.1 GPa to carry out cooling runs (see next section), but on increasing pressure through 0.15 GPa on the following days, the same behavior was observed (see inset in Fig. 4). It thus seems unlikely that this is a random phenomenon caused by the cell geometry or technical problem.

Between 0.2 and 0.5 GPa, the resistance drops smoothly but rather rapidly with increasing pressure, but above this the curve flattens out. Isothermal pressure runs show that, to a reasonable approximation, the room temperature resistance decreases exponentially with increasing pressure until it becomes almost pressure independent above 1.5–2 GPa. In one experiment, we even observed a slight increase in R with increasing pressure above 1.5 GPa, but this could be an effect of changes in geometrical factors.

The compressibility of Rb_4C_{60} has been studied in two recent papers,^{17,18} and structural transitions have been found in the range of 0.4–0.8 GPa. Sabouri-Dodaran *et al.*¹⁷ claimed the existence of a sharp isostructural first-order transition between 0.5 and 0.8 GPa, while Huq and Stephens¹⁸ interpreted their data as indicating a transformation from an orientationally disordered tetragonal structure to an orientationally ordered orthorhombic structure over a range in pressure below 0.5 GPa. The absence of any sharp anomalies in our data up to 2 GPa and the fact that the resistance drops more rapidly below 0.5 GPa indicate that our data are in better agreement with the results of Huq and Stephens than

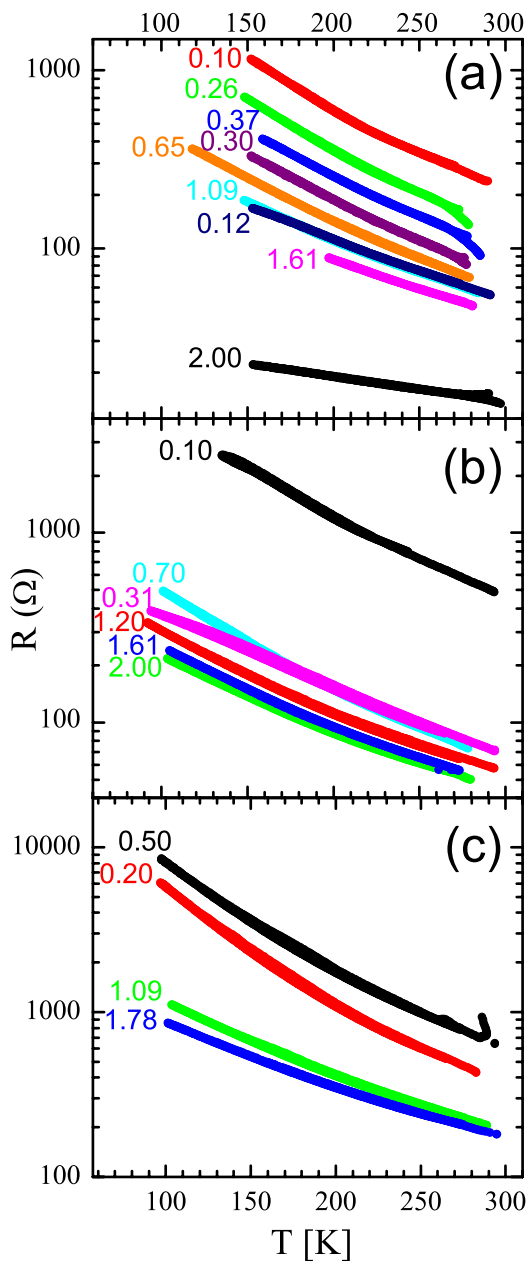


FIG. 5. (Color online) Isothermal temperature dependence of the resistance of Rb_4C_{60} under pressure. (a)–(c) show results from the three separate experiments. The curves for each sample (subfigure) are labeled with the pressures (in gigapascals) at which they were measured. The chronological order of acquisition was in (a) 0.10, 0.26, 0.37, 1.09, 1.61, 0.65, 0.30, 0.12, and 2.00 GPa, in (b) 0.10, 1.20, 2.00, 1.61, 0.70, and 0.31 GPa, and in (c) 0.50, 1.78, 1.09, and 0.20 GPa pressure.

those of Sabouri-Dodaran *et al.* The smooth drop in resistance (by a factor of 3–5) over the range of 0.2–0.5 GPa should not be incompatible with small changes in band gap, gap structure, and phonon spectrum caused primarily by orientational ordering of the fullerene molecules. Anomalies with a similar magnitude are observed at the orientational ordering transition in pure C_{60} .^{15,29,30}

It was obvious already from the data obtained in the first experiment that the results did not support the existence of an insulator-to-metal transformation in the pressure range studied here at least not at room temperature and below. In the second and third experiments, we therefore extended the available temperature range to include also temperatures above room temperature.

2. Resistance versus temperature at high pressure

In the course of each experiment, we carried out isobaric temperature scans at a number of pressures. Selected results for $R(T)$ obtained during temperature scans below room temperature in the three experiments are shown in Figs. 5(a)–5(c). The logarithmic resistance scale of the plots clearly shows that the sample resistance in each case varies nearly exponentially with temperature, and that the temperature coefficient of the resistance is negative. Different absolute values of R are a consequence of different sample amounts and geometries, as well as the dependence of resistivity on pressure and changes in the sample structure (to be discussed in more detail below). As evidenced by Fig. 5, a semiconducting behavior was clearly observed at all pressures in this study. Furthermore, no significant differences were observed in the relative temperature dependence between experiments nor at different pressures. We can therefore repeat and emphasize the statement already given above that no insulator-metal phase transition is observed in Rb_4C_{60} up to 2 GPa. This somewhat disappointing result clearly contradicts the conclusions from earlier NMR studies.^{14,31}

Already our first attempts to analyze the data obtained in the isobaric cooling runs showed that a simple semiconductor model was not able to provide a satisfactory fit to the data. Because the sample was known to be granular, we then tried to employ a hopping conduction model. This gave rather good results, but only over the limited temperature range below room temperature, and even in this range clear deviations were observed at the temperature extremes. After extending the temperature range by adding the heating facility, neither of the models mentioned could be used to analyze the data over the full temperature range of the experiments. In fact, a quite good fit could be obtained using a single exponential dependence on temperature [notice that the $R(T)$ curves shown on the logarithmic scale in Fig. 5 are nearly straight lines]. Obviously, such a model is incompatible with a standard semiconducting behavior where an exponential in T^{-1} is expected.

Closer analysis reveals that the resistivity of Rb_4C_{60} in fact shows the same general behavior as most fullerene-based materials. It is well known that the resistance of pure C_{60} under vacuum conditions shows two types of behavior.³² At room temperature and below, the resistivity of C_{60} follows the standard semiconductor “law,”

$$\rho = \rho_0 \exp(E_g/2k_B T), \quad (1)$$

with an effective band gap value E_g of about 0.4 eV, much smaller than the optically measured band gap. [Equation (1) is often simplified by substitution of an activation energy $E_a = E_g/2$.] Well above room temperature, the activation energy becomes much higher and agrees well with the actual

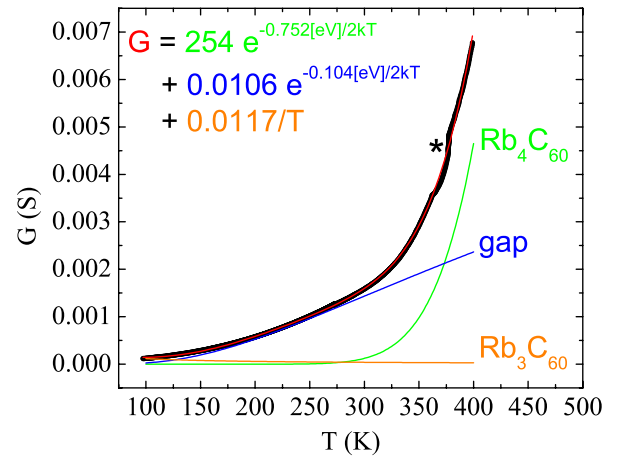


FIG. 6. (Color online) A typical set of data for the conductance G of a nominal Rb_4C_{60} sample with a theoretical fit to Eq. (2) (red curve) and its three components, attributed to metallic Rb_3C_{60} (orange) and Rb_4C_{60} (gap states blue, intrinsic gap green), as labeled. Asterisk (*) marks the region where the resistance data were affected by the phase transformation of Teflon (see text).

band gap measured optically. For samples containing oxygen, on the other hand, the low-temperature resistivity is significantly higher and the temperature dependence is governed by an E_g very close to the actual band gap.^{29,30,32} It is believed that the low “vacuum” value of E_g is due to states in the gap which are eliminated by reaction with oxygen.

A very similar behavior is observed for our samples, although modified by an additional term at low temperatures. As in the case of pure C_{60} , the total conductance G of Rb_4C_{60} can be written as the sum of two semiconductor conductances with different activation energies (or band gaps), corresponding to carriers thermally activated from the valence band to the conduction band and from (or to) states in the gap, respectively. We can consider these as corresponding to “intrinsic” conduction and to “doping” by defects (self-doping). Because we could detect the presence of a small fraction of Rb_3C_{60} in our samples after the experiments, we have added a “metallic” conductance proportional to T^{-1} to account for the additional low-temperature term observed. (In principle, conduction in mixed samples is a very complex problem but as long as the fraction of metallic phase is small a simple additive term seems sufficient to model the behavior.) Because this term is small and only important at the lowest temperatures, we could have obtained equally good fits adding instead a third semiconductor term or a constant. The latter model would be unphysical, but adding a third semiconductor would be a way to simulate a more realistic broad distribution of gap states. However, adding another adjustable parameter would also increase the scatter in the data. The model used can thus be written as

$$G(T) = C_{\text{Rb}_4\text{C}_{60}} \exp[-E_g^{\text{Rb}_4\text{C}_{60}}/2k_B T] + C_{\text{gap}} \exp[-E_g^{\text{gap}}/2k_B T] + C_{\text{Rb}_3\text{C}_{60}}/T, \quad (2)$$

where $E_g^{\text{Rb}_4\text{C}_{60}}$ and E_g^{gap} are the two energy gaps of Rb_4C_{60} ,

respectively, and C_x are the “conductance amplitudes” of each term, including information about the relative amounts, the sample geometry and the conductivities. It should be noted that this model is strictly valid at isochoric (constant volume) conditions, while data were collected under isobaric conditions. Since the equation of state is not known for Rb_4C_{60} over most of the range investigated, we cannot carry out the corresponding corrections, and following standard practice we have fitted Eq. (2) directly to the measured data.

With this model, it was possible to obtain a good fit to all data collected in the range of 90–420 K. A set of wide temperature range $G(T)$ data, together with a fit of the two-semiconductors-and-one-metal model of Eq. (2) is shown in Fig. 6. The fitted function has also been decomposed into its three components to show that the measured conductivity is dominated by carriers excited from gap states over most of the temperature range studied, except at very low and very high temperatures. However, the high number of adjustable parameters means that even small errors in the data may cause large shifts in the fitted parameters, and the possible errors in the fitted parameters may be rather large. Also, in our experiments, the accessible ranges of temperatures within which the total G contains a significant fraction from either metallic Rb_3C_{60} or from the “intrinsic” conductivity of Rb_4C_{60} are very limited, causing a larger scatter in the corresponding fitted parameters as compared to those for “self-doped” Rb_4C_{60} . For the majority of the temperature runs, extending only below room temperature, we have therefore also fitted a simplified model using only the two last terms in Eq. (2). These fits give a smaller scatter in the fitted parameters for the gap state conductivity, but it is obvious from both the plotted fit results and from a comparison with the fits to the complete Eq. (2) that they overestimate slightly both the metallic term and the fitted energy gaps E_g^{gap} , such that the latter are 10–20 meV higher than the values obtained from fits of the full Eq. (2). The data set shown in Fig. 6 was also selected because it shows the typical size of the anomalies sometimes observed at the phase transitions of the Teflon™ pressure medium.

Based on the fits obtained for the experimental data sets measured over the widest temperature range (about 100–400 K), we estimate the effective energy gaps E_g in Eq. (2) for Rb_4C_{60} at normal pressure to be 0.11 ± 0.01 eV (gap states) and 0.7 ± 0.1 eV (intrinsic band gap), respectively. The errors are based on the scatter in the fitted parameters only, and the real uncertainties might be greater. Despite the fact that the energy gap values are obtained in a rather crude way, the magnitudes are very reasonable. The band gaps of Rb_4C_{60} , measured by electron energy loss spectroscopy¹¹ and optical reflectivity,³³ are given as 0.6 ± 0.1 eV and about 0.5 eV, respectively, in very good agreement with our result. In view of the possibility of an insulator-to-metal transition in Rb_4C_{60} , we have also tried to estimate how its intrinsic energy gap depends on pressure. However, due to the limitations discussed above random fluctuations in the fitted results are larger than systematic trends, and although there is possibly a weak decrease in the band gap up to 2 GPa, with a pressure dependence comparable to that for C_{60} ,¹⁵ there should be no insulator-metal transition arising from a continuous closing of the intrinsic band gap until well above 10 GPa.

Returning to the gap states, we found that for Rb_4C_{60} carriers derived from these states are excited over a gap of about 0.11 eV. This value is of the same order of magnitude as for other fullerene-based materials,^{15,29,30,32} and we note that NMR data of Zimmer *et al.*²⁵ also show electrons to be excited over a gap of about 100 meV in Rb_4C_{60} , in excellent agreement with our result. For pure C_{60} , the corresponding levels are deeper^{29,30,32} at 0.3–0.8 eV below the conduction band. Also, in this case, the states can be eliminated by the presence of oxygen,^{29,32} and the energies depend on pressure³⁰ and on the rotational state of the molecules^{29,30} such that E_a is higher for freely rotating molecules and decreases with increasing pressure. For Rb_4C_{60} , we obviously cannot test the oxygen sensitivity, but our data show that E_g^{gap} decreases with increasing pressure. A linear fit to all data for E_g^{gap} versus pressure indicates a slope of approximately -0.02 eV GPa⁻¹, rather similar to that in C_{60} ,¹⁵ and indicating that it might reach zero above 6 GPa. The data are also compatible with a more speculative interpretation in terms of a constant low-pressure value of 0.11 eV up to about 0.5 GPa, a decrease by $15 \pm 5\%$ in the range where Huq and Stephens¹⁸ found an orientational ordering of the C_{60} molecules, and above 0.5 GPa a quite slow decrease with increasing pressure. Such a behavior would indicate that the gap states could be associated with the orientational and/or rotational state of the C_{60} molecules, as in pure fullerenes. However, the scatter in the data is very high and the linear interpretation is preferable from a statistics point of view. As far as we know, Rb_4C_{60} has never been studied above 5.2 GPa,¹⁷ and further studies at very much higher pressures are obviously needed in order to finally answer the questions about the possible insulator-to-metal transition in this material.

Finally, from the data of Huq and Stephens,¹⁸ we see that the material starts out in the body-centered tetragonal, orientationally disordered state and transforms into an orthorhombic, orientationally ordered phase. However, the lattice parameters compress at different rates under pressure, and near 1.6 GPa, two parameters are again equal, giving again an effectively tetragonal structure. We have thus chosen to make temperature runs at this pressure in two of our experiments. However, within the accuracy of the data, the fitted band gaps and other properties vary smoothly with pressure above 1 GPa, with no particular effect observed at 1.6 GPa. From the result presented above, we can speculate that the orientational disorder seems to have a larger effect on at least the observed gap states than the actual lattice structures (which are, admittedly, very similar).

For the two “control” samples, nominally pure Rb_6C_{60} and the mixed Rb_xC_{60} sample ($x=3, 4,$ and 6), the resistance versus temperature curves were superficially very similar to those for Rb_4C_{60} , and thus again dominated by gap states. For Rb_6C_{60} , the average fitted gap state energy E_g^{gap} was found to be about 65 meV and thus lower than for Rb_4C_{60} . The band gaps of the A_6C_{60} compounds are not well known and estimates for K_6C_{60} range from 0.5 (Ref. 34) to 1.7 eV.³⁵ The four fitted values for the intrinsic band gap of Rb_6C_{60} were rather scattered but indicate a value of (0.5 ± 0.1) eV, rather lower than expected. The pressure dependence could not be determined for either the band gap or the gap state

energy due to the large scatter and the small number of data points. For the mixed sample, the conductivity was again dominated by the gap states of Rb_4C_{60} and by (metallic) conduction in Rb_3C_{60} . The data for these samples thus did not give much additional information and will not be discussed further here.

3. Time dependence

In all three experiments, we have observed a time-dependent decrease in the total resistance of the samples, superimposed on the changes with pressure and temperature. Although we would expect that the resistance would be a stable and repeatable function of pressure and temperature after the initial compression of the powder has taken place (over the first few hundred megapascals), possibly with some minor changes due to changes in the geometrical factors, we have actually observed a continuous decrease in the sample resistance with time throughout each experiment, superimposed on the intrinsic pressure dependence (see the chronological order of the curves in Fig. 5). The largest changes occurred after heating to above 400 K and when decreasing the pressure below 0.5 GPa after measurements at the highest pressures, but there were also noticeable changes in R with time while the samples were resting close to room temperature after being heated from low temperatures. Apart from a possible slow insulator-to-metal transition in Rb_4C_{60} , for which we have found no evidence, there are at least three possible explanations for such a phenomenon: the material may simply lose Rb to transform into (metallic) Rb_3C_{60} , the Rb_4C_{60} may separate into Rb_3C_{60} and Rb_6C_{60} , or pressure and/or temperature treatment may create more gap states, possibly by introducing structural defects in the sample.

To distinguish between these possibilities, the most direct way would be to characterize the samples again after the experiments. However, due to the small sample size and difficulties encountered when opening the pressure cells and transferring the samples into capillaries inside the glovebox, this was not always possible and, as will be shown in Sec. III B, the samples from the last two experiments were also destroyed by other effects before the end of the experiments. We have, therefore, instead tried to draw conclusions from the parameters obtained from fitting Eq. (2) to the data from each temperature scan. This analysis shows that the general behavior was the same in all three experiments. As long as the temperature did not exceed room temperature, the conductivity magnitude of the “metallic” part was within the experimental error a quasilinear, reversible function of pressure until the pressure was decreased to below about 0.4 GPa. Below this, it increased with decreasing pressure, indicating formation of Rb_3C_{60} . A similar increase in the metallic term was observed after heating to above about 420 K. It was thus clear that during most of the experiments the dominant source of the observed resistance drift was an increase in the “gap state” term of Eq. (2). We believe that this increase is due to the creation of defect states in the material when it is deformed during changes of pressure and temperature. Cooling and heating of the pressure vessel are associated with volume changes due to thermal contraction and expansion, mainly of the pressure medium. Even if the

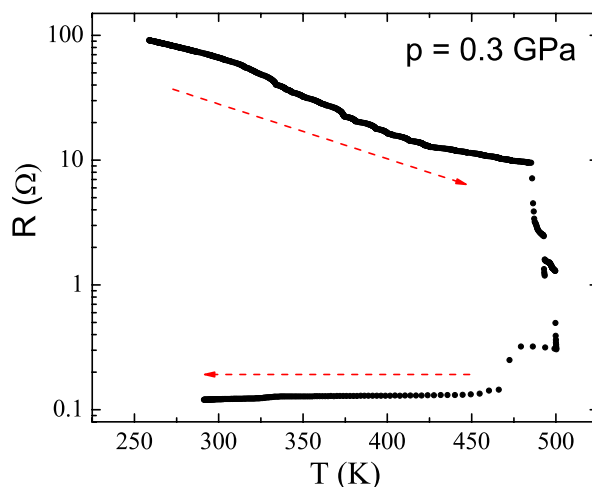


FIG. 7. (Color online) Resistance of second (initially Rb_4C_{60}) sample on heating to 500 K, showing an insulator-to-metal transition. Dashed arrows indicate the direction of temperature change.

applied force is kept constant and friction is minimized by the choice of materials and a liberal application of lubricant, such volume changes unavoidably gives rise to systematic variations in pressure during temperature scans. During each temperature scan, the samples are thus cyclically deformed, probably leading to a continuous increase in the density of defects in the sample with time. We believe that this mechanism greatly increases the defect density and thus also the density of gap states in the samples, causing most of the time-dependent changes (drift) in the resistance of the samples. This also implicitly means that we identify the gap states with defect states due to positional and orientational disorder. Although Huq and Stephens¹⁸ found the high-pressure state to be orientationally ordered, nonhydrostatic pressure conditions and sample deformation probably create both types of disorder in the material. As for the metallic term, there is a clear additional increase when the pressure is reduced below 0.4 GPa, suggesting a link to the ordering transition observed by Huq and Stephens.¹⁸ If this transformation is reversible, the strong lattice deformation suffered by the sample under pressure may frustrate the reverse transformation into the tetragonal zero-pressure phase, causing a strong increase in the number of both positional and orientational defects.

The source of the observed increase in metallic conductivity at low pressures is more elusive. If this term is really due to Rb_3C_{60} in the samples, Rb loss from reactions with remaining water or oxygen in the cell is a possible explanation for at least part of the effect seen on heating to 420 K since high temperature increases the diffusion rates, but does not explain the effect noticed on decreasing pressure to below 0.5 GPa. Heating at zero pressure caused a large effect; in this case, it may be possible (but unlikely) that some water or air may have entered the pressure cell, but this should not happen as long as a load is applied by the press.

In principle, phase separation of Rb_4C_{60} into Rb_3C_{60} and Rb_6C_{60} should also be possible. A simple density calculation based on the known unit cell parameters²² shows that such a

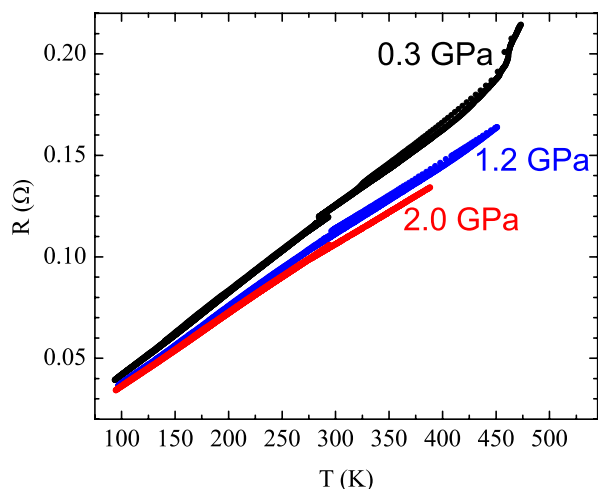


FIG. 8. (Color online) Resistance of the sample after the metalization shown in Fig. 7, measured during isobaric temperature scans at the pressures as indicated.

phase separation would increase the average density by 4%, which is clearly favorable under high pressure and may lead to a phase separation driven by the pressure-volume (pV) term in the energy. However, we would then expect that the separation should be faster at the highest pressure or whenever the number of defects has been increased by deformation of the sample, and the fact that the metallic conductivity is reversible at the highest pressures clearly speaks against this mechanism. Again, the increase in the fraction of Rb_3C_{60} on decreasing pressure below 0.4 GPa may be linked to a partially frustrated transformation, causing not only a strong increase in the number of defects but perhaps also an increased number of diffusion paths or an increased possibility for phase separation.

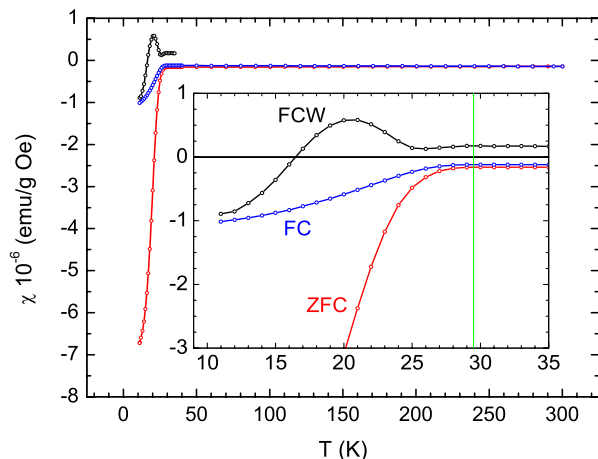


FIG. 9. (Color online) Low-temperature magnetic susceptibility for the sample shown in Figs. 7 and 8, measured by a SQUID magnetometer. The inset shows an enlargement of the transition region. The three curves show zero-field cooled (ZFC, red), field-cooled (FC, blue) and field-cooled low-field warming-up (FCW, black) temperature scans. The green vertical line on the inset indicates the nominal onset temperature of the superconducting transition in Rb_3C_{60} .

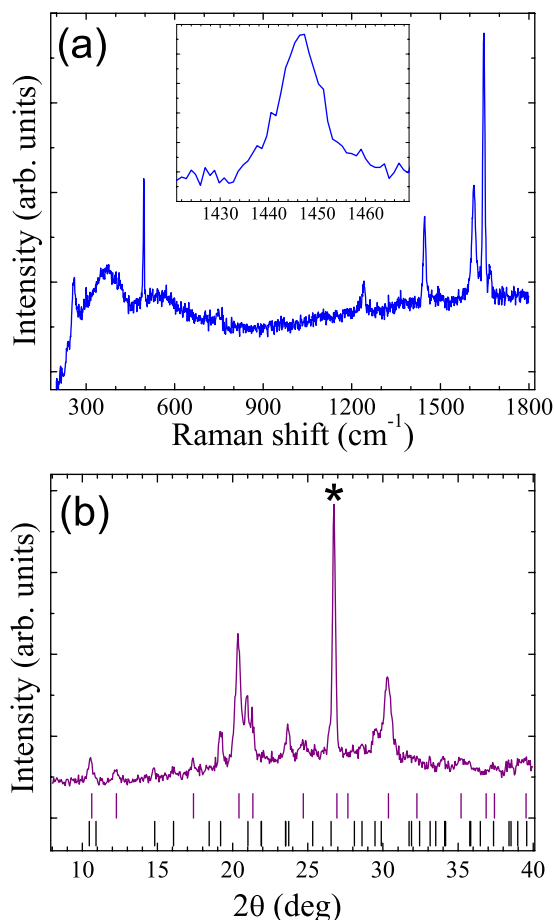


FIG. 10. (Color online) (a) Raman data and (b) XRD results for an initially Rb_4C_{60} sample transformed by heating. Inset in (a) shows the $A_g(2)$ mode on an expanded energy scale. Peak marked by asterisk in (b) is from the BN pressure medium; ticks show expected line positions for Rb_3C_{60} (upper row, purple) and Rb_4C_{60} (lower row, black) calculated from literature data (Ref. 22).

As mentioned above, at least part of this term could also be due to formation of gap states with a very small excitation energy. In such a case, the reversible variation with pressure probably corresponds to large relative shifts in the energies with pressure while the permanent low pressure changes are again due to creation of further defects.

B. Effects of high-temperature treatment

At the end of the second high-pressure experiment, we decided to investigate whether an insulator-to-metal transition could be provoked by heating, and we therefore slowly brought the sample to a temperature of 500 K at 0.3 GPa. As shown in Fig. 7, just below 500 K the resistance of the nominally Rb_4C_{60} sample decreased rapidly by a significant fraction, indicating a sharp transition into a new state. On cooling, the low resistance state persisted to room temperature. In the hope that this was indeed the metallic state of Rb_4C_{60} , we carried out another set of high pressure studies over a similar range of temperatures to characterize the material. Figure 8 shows selected results, indicating a metallic state with a re-

sistance linear in temperature and with a weak pressure dependence above 0.3 GPa and a temperature coefficient typical for metals, about $3.1 \times 10^{-3} \text{ K}^{-1}$ at 0.3 GPa and 300 K. (No accurate zero-pressure data could be obtained since one of the connecting wires broke on decreasing pressure.) The second, mixed state sample in the cell also showed a large drop in resistance magnitude, but no metallic state appeared after heating. The same type of treatment was also carried out at the end of the third high-pressure experiment. Surprisingly, in this case, an originally Rb_6C_{60} sample transformed into a metallic state, while the initially Rb_4C_{60} retained its semiconducting character, although with a reduced resistivity.

After the experiments, we removed the very small samples from the pressure cell for characterization. The results clearly showed that the samples now contained Rb_3C_{60} as majority phase. Figure 9 shows that the onset of the superconducting transition for the material falls at 29 K, in excellent agreement with data for Rb_3C_{60} .^{5,36} The relatively low bulk transition temperature near 20 K and the wide transition range indicates that the bulk of the material has a non-uniform composition and/or very small grains. This is compatible with the observation of a paramagnetic behavior in the superconducting state (Wohleben or paramagnetic Meissner effect) in a very weak field (100 G), a feature usually shown by disordered materials with very small grains.³⁷

Figure 10 shows Raman and XRD data for the initially Rb_4C_{60} sample from the third experiment. The Raman data show a strong $A_g(2)$ mode at 1447 cm^{-1} and other features characteristic for Rb_3C_{60} , and although the strongest peaks for Rb_4C_{60} are clearly seen in the XRD diagram, it is dominated by peaks from Rb_3C_{60} . No trace of Rb_6C_{60} is observed by either method.

The transformation observed is rapid, and the absence of Rb_6C_{60} in the samples after the experiments indicates that the phase separation process discussed above is not responsible. Instead, the samples seem to have lost Rb by a rapid process. Again, it may be possible that some water or oxygen is present in the cell, but the sudden onset and rapid transformation speak against reaction with impurities already present at lower temperatures. Instead, the “transition temperature” correlates well with the 460 K melting point of the Sn-Pb solder used to attach the Ni contact probes to the Cu wires. Rb is known to react with both Sn and Pb.³⁸ Although the solder was applied several millimeters from the samples, it is possible that capillary action has brought liquid Sn-Pb alloy into contact with the sample, making a reaction between Rb and Sn or Pb possible such that Rb diffused out of our samples. In fact, a very thin solder film was observed to

have spread between the Teflon layers in certain areas when the last pressure cell was opened. This mechanism also explains the random element of the transformation, i.e., why only some samples, with different compositions, transformed.

IV. CONCLUSIONS

We have presented the results of direct resistance measurements on Rb_4C_{60} under pressure. We show that our data are compatible with recent structural studies but, in contradiction of an earlier NMR result, we find that there is no insulator-to-metal transition up to a pressure of 2 GPa. Our conductivity data can be fitted with excellent results to a model consisting of two semiconducting and one metallic channels acting in parallel, and interpreted in terms of (at least) two phases, one metallic and the other a semiconductor with gap donor states. The model is consistent with the sample composition and with known fullerene properties and has a good physical background. The estimated energy gap(s) and their behavior under pressure are in agreement with the expected properties of the material, but although the gap decreases slightly with increasing pressure, we see no indications of an incipient closing of the band gap under high pressure. However, the already high zero-pressure conductivity of Rb_4C_{60} , dominated by self-doping by gap states, increases by more than an order of magnitude through the ordering transition and up to 1 GPa. It is possible that the earlier report¹⁴ of an insulator-metal transition in this material was based on the high conductivity of this self-doped semiconductor. Although some of our samples showed a transition to a metallic behavior under pressure after high-temperature treatment, this was clearly identified as a consequence of rapid loss of Rb from the samples, causing a transformation to metallic Rb_3C_{60} . As far as we know, Rb_4C_{60} has never been studied above 5.2 GPa,¹⁷ and further studies at very much higher pressures are needed in order to finally answer the questions about the possible insulator-to-metal transition in this material, especially in view of the fact that the related compound Na_2C_{60} also is known to have a phase transformation into a little known state under relatively low pressures.³⁹

ACKNOWLEDGMENTS

This work was financially supported by the Swedish Research Council. T.W. also thanks the Wenner-Gren Foundations for generous support.

*Present address: Department of Materials, University of Oxford, Parks Road, Oxford OX1 3PH, United Kingdom.

¹R. C. Haddon, A. F. Hebard, M. J. Rosseinsky, D. W. Murphy, S. J. Duclos, K. B. Lyons, B. Miller, J. M. Rosamilia, R. M. Fleming, A. B. Kortan, S. H. Glarum, A. V. Makhija, A. J. Muller, R. H. Eick, S. M. Zahurak, R. Tycko, G. Dabbagh, and F. A. Thiel,

Nature (London) **350**, 320 (1991).

²D. W. Murphy, M. J. Rosseinsky, R. M. Fleming, R. Tycko, A. P. Ramirez, R. C. Haddon, T. Siegrist, G. Dabbagh, J. C. Tully, and R. E. Walstedt, J. Phys. Chem. Solids **53**, 1321 (1992).

³D. M. Poirier, D. W. Owens, and J. H. Weaver, Phys. Rev. B **51**, 1830 (1995).

- ⁴A. F. Hebard, M. J. Rosseinsky, R. C. Haddon, D. W. Murphy, S. H. Glarum, T. T. M. Palstra, A. P. Ramirez, and A. B. Kortan, *Nature (London)* **350**, 600 (1991).
- ⁵K. Holczer, O. Klein, S. M. Huang, R. B. Kaner, K. J. Fu, R. L. Whetten, and F. Diederichs, *Science* **252**, 1154 (1991).
- ⁶R. M. Fleming, M. J. Rosseinsky, A. P. Ramirez, D. W. Murphy, J. C. Tully, R. C. Haddon, T. Siegrist, R. Tycko, S. H. Glarum, P. Marsh, G. Dabbagh, S. M. Zahurak, A. V. Makhija, and C. Hampton, *Nature (London)* **352**, 701 (1991).
- ⁷F. Stepniak, P. J. Benning, D. M. Poirier, and J. H. Weaver, *Phys. Rev. B* **48**, 1899 (1993).
- ⁸G. Oszlányi, G. Baumgartner, G. Faigel, and L. Forró, *Phys. Rev. Lett.* **78**, 4438 (1997).
- ⁹S. Margadonna, D. Pontiroli, M. Belli, T. Shiroka, M. Riccò, and M. Brunelli, *J. Am. Chem. Soc.* **126**, 15032 (2004).
- ¹⁰R. Röding, T. Wågberg, and B. Sundqvist, *Chem. Phys. Lett.* **413**, 157 (2005).
- ¹¹M. Knupfer and J. Fink, *Phys. Rev. Lett.* **79**, 2714 (1997).
- ¹²V. Brouet, H. Alloul, S. Gàràj, and L. Forró, *Struct. Bonding (Berlin)* **109**, 165 (2004).
- ¹³G. Klupp, K. Kamaras, N. M. Nemes, C. M. Brown, and J. Leão, *Phys. Rev. B* **73**, 085415 (2006).
- ¹⁴R. Kerkoud, P. Auban-Senzier, D. Jérôme, S. Brazovskii, I. Luk'yanchuk, N. Kirova, F. Rachdi, and C. Goze, *J. Phys. Chem. Solids* **57**, 143 (1996).
- ¹⁵B. Sundqvist, in *Fullerenes: Chemistry, Physics, and Technology*, edited by K. M. Kadish and R. S. Ruoff (Wiley, New York, 2000), pp. 611–690.
- ¹⁶B. Sundqvist, *Struct. Bonding (Berlin)* **109**, 85 (2004).
- ¹⁷A. A. Sabouri-Dodaran, M. Marangolo, Ch. Bellin, F. Mauri, G. Fiquet, G. Louprias, M. Mezouar, W. Crichton, C. Hérold, F. Rachdi, and S. Rabii, *Phys. Rev. B* **70**, 174114 (2004).
- ¹⁸A. Huq and P. W. Stephens, *Phys. Rev. B* **74**, 075424 (2006).
- ¹⁹A. A. Sabouri-Dodaran, Ch. Bellin, M. Marangolo, G. Louprias, S. Rabii, F. Rachdi, Th. Buslaps, and M. Mezouar, *Phys. Rev. B* **72**, 085412 (2005).
- ²⁰C. A. Kuntscher, G. M. Bendele, and P. W. Stephens, *Phys. Rev. B* **55**, R3366 (1997).
- ²¹J. P. McCauley, Jr., Q. Zhu, N. Coustel, O. Zhou, G. Vaughan, S. H. J. Idziak, J. E. Fischer, S. W. Tozer, D. M. Groski, N. Bykovetz, C. L. Lin, A. R. McGhie, B. H. Allen, W. J. Romanow, A. M. Denenstein, and A. B. Smith, *J. Am. Chem. Soc.* **113**, 8537 (1991).
- ²²P. W. Stephens, L. Mihaly, J. B. Wiley, S.-M. Huang, R. B. Kaner, F. Diederich, R. L. Whetten, and K. Holczer, *Phys. Rev. B* **45**, 543 (1992).
- ²³R. C. Haddon, A. S. Perel, R. C. Morris, S.-H. Chang, A. T. Fiory, A. F. Hebard, T. T. M. Palstra, and G. P. Kochanski, *Chem. Phys. Lett.* **218**, 100 (1994).
- ²⁴J. Reichenbach, F. Rachdi, I. Luk'yanchuk, M. Ribet, G. Zimmer, and M. Mehring, *J. Chem. Phys.* **101**, 4585 (1994).
- ²⁵G. Zimmer, M. Mehring, C. Goze, and F. Rachdi, *Phys. Rev. B* **52**, 13300 (1995).
- ²⁶A. Iwasiewicz-Wabnig, B. Sundqvist, É. Kováts, I. Jalsovszky, and S. Pekker, *Phys. Rev. B* **75**, 024114 (2007).
- ²⁷C.-K. Wu and M. Nicol, *Chem. Phys. Lett.* **21**, 153 (1973).
- ²⁸W. A. Vareka and A. Zettl, *Phys. Rev. Lett.* **72**, 4121 (1994).
- ²⁹T. Arai, Y. Murakami, H. Suematsu, K. Kikuchi, Y. Achiba, and I. Ikemoto, *Solid State Commun.* **84**, 827 (1992).
- ³⁰S. Matsuura, T. Ishiguro, K. Kikuchi, Y. Achiba, and I. Ikemoto, *Fullerene Sci. Technol.* **3**, 437 (1995).
- ³¹R. Kerkoud, P. Auban-Senzier, D. Jérôme, S. Brazovskii, N. Kirova, I. Luk'yanchuk, F. Rachdi, and C. Goze, *Synth. Met.* **77**, 205 (1996).
- ³²T. L. Makarova, *Semiconductors* **35**, 243 (2001).
- ³³Y. Iwasa and T. Kaneyasu, *Phys. Rev. B* **51**, 3678 (1995).
- ³⁴S. C. Erwin and M. R. Pederson, *Phys. Rev. Lett.* **67**, 1610 (1991).
- ³⁵G. K. Wertheim and D. N. E. Buchanan, *Phys. Rev. B* **47**, 12912 (1993).
- ³⁶V. Buntar, in *Fullerenes: Chemistry, Physics, and Technology*, edited by K. M. Kadish and R. S. Ruoff (Wiley, New York, 2000), pp. 691–766.
- ³⁷W. Braunisch, N. Knauf, V. Kataev, S. Neuhausen, A. Grütz, A. Kock, B. Roden, D. Khomskii, and D. Wohlleben, *Phys. Rev. Lett.* **68**, 1908 (1992); A. K. Geim, S. V. Dubonos, J. G. S. Lok, M. Henini, and J. C. Maan, *Nature (London)* **396**, 144 (1998); M. S. Li, *Phys. Rep.* **376**, 133 (2003).
- ³⁸I. F. Hewaidy, E. Busmann, and W. Klemm, *Z. Anorg. Allg. Chem.* **328**, 283 (1964).
- ³⁹T. Yildirim, D. A. Neumann, S. F. Trevino, and J. E. Fischer, *Phys. Rev. B* **60**, 10707 (1999).